

MILP based Optimal Design of Hybrid Microgrid by Considering Statistical Wind Estimation and Demand Response

E. Naderi, A. Dejamkhooy*, S.J. Seyedshenava, H. Shayeghi

Department of Electrical Engineering, University of Mohaghegh Ardabili, Ardabil, Iran

Abstract-Recently due to technical, economical, and environmental reasons, penetration of renewable energy resources has increased in the power systems. On the other hand, the utilization of these resources in remote areas and capable regions as isolated microgrids has several advantages. In this paper, a hybrid microgrid, which includes photovoltaic (PV)/wind/energy storage, is investigated. It has been located in Iran-Khalkhal. The purposes of this study are optimal energy management and sizing of the microgrid. Since the magnitude of the harvested renewable energy deals severely and complexly with season and climate issues, planning of the system based on their specific values is an oversimplification. Therefore, in addition to conventional constraints such as environmental and operational ones, estimation of the wind speed at the site is considered. The Monte Carlo method is employed to model and estimate wind behavior. Also, for regulating production and demand in the microgrid the Demand Response (DR) program is conducted to improve the contribution of the renewable energy resources. The planning is constructed as an optimization problem. It is formulated as a Mixed Integer Linear Programming (MILP). By solving it, the size and production magnitude of energy sources, as well as storage conditions, are determined. Finally, the proposed method is simulated by GAMS for all seasons of two scenarios. The results show desirable energy management and cost reduction in the studied grid.

Keyword: Demand Response, Hybrid Microgrid, Monte Carlo method, Mixed integer linear programming, Wind speed model.

1. INTRODUCTION

All life on earth depends in some way upon energy. The energy demand is increasing rapidly across the world. Today, it comes from renewable and non-renewable resources. Fossil fuels, as a part of non-renewable resources, seriously affect the environment. Also, it needs money for extraction from the ground, processing, and transportation to the end-user. Besides, the shortage of these resources has raised their prices. Also, there is a significant shortage of power supply in remote areas such as rural and island areas [1]. Therefore, the world needs some significant energy production modifications. The previously mentioned challenges lead the decision-makers to think about a small-scale and decentralized group of electricity sources named HMGS. These can operate independently from power grids and provide electricity to a remote location. HMGS, including WT and PV, is an excellent solution for electrification while

ensuring high reliability [2]. Furthermore, ESS is utilized as a system backup for compensating the intermittency and variability of RES. The first step design of HMGS is an investigation of the meteorological conditions to extract maximum wind and solar energy. The meteorological data, like wind speed and solar radiation, are dependent on weather conditions and geographical characterization. Therefore, weather forecasts are necessary to establish the optimal planning of MG systems. In Ref. [3], a general overview of the meteorological data effects on MGs was provided. This paper focused on the implementation of weather forecasts in MG energy management systems. As mentioned in this paper, a desirable test period is one year or at least three or four days with different meteorological situations. In Ref. [4], the forecasted meteorological impacts on fuel consumption and energy storage requirement were investigated.

Numerous methods have been stated to overcome the challenges of wind speed forecasting. These methods utilized statistics, machine learning, and the majority of those are data-driven. For instance, in Ref. [5] multilayer feed-forward neural network (MLFFNN), support vector regression with a radial basis function (SVR-RBF), adaptive neuro-fuzzy inference system

Received: 11 Jan. 2021

Revised: 16 May 2021

Accepted: 17 May 2021

*Corresponding author:

E-mail: majiddejam@uma.ac.ir (A. Dejamkhooy)

DOI: 10.22098/joape.2022.8271.1572

Research Paper

© 2022 University of Mohaghegh Ardabili. All rights reserved.

optimized with a partial swarm optimization algorithm (ANFIS-PSO) are discussed to predict wind speed. In Ref. [6], a combination of mutual information, wavelet transform, evolutionary PSO, and the adaptive neuro-fuzzy inference system for wind power forecasting has been presented. Other methods that have been discussed are based on the use of polynomial autoregression [7], and Gaussian processes (GP) with PSO [8], and kernel modeled Gaussian processes with a fuzzy driven multiplexer [9]. But these methods are very complicated and time-consuming, especially when the number of input variables is large. The area available for MG installations is another constraint for the optimal design of MG. We term it Available Space constraint. Determination of the maximum capacity of the HMGS is necessary for the optimal design of the HMGS. It is limited by the load demand on the site, the primary investment, and the available area [10-11].

Therefore, the area used by PV and WT must be considered. The maximum harvesting and management of RES are the next step in the planning of the MG system. Researchers have done many studies to minimize the energy production costs and optimal planning of hybrid MG systems. The optimum economic operation of MG, including thermal and electrical energy, through a bi-objective optimization model, has been investigated [12]. The fuzzy epsilon decision is employed for converting a bi-objective function to a single objective function. In Ref. [13], the generation cost and pollutant emission have been considered as objective functions. A recently developed Crow Search Algorithm (CSA) has been implemented to execute the optimization. The authors have compared the obtained results by several different soft computing techniques such as GA and PSO algorithms. In Ref. [14], a mathematical model has been proposed for the MG generation cost function. The load has been considered to be variable and unpredictable. To reduce costs, an economic strategy based on forecasting has been proposed by using the neural network. Besides, optimal load distribution has been calculated by economic analysis [15].

An overview of advanced methods for modeling the uncertainty in the distribution network design has been conducted [16]. In Ref. [17], operational cost and environmental pollution are formulated as the objective functions. The Multi-Objective Group Search Optimization algorithm solved the energy management problem. Forecasted values of uncertain parameters are utilized to generate a two-dimensional conditional PDF using a copula. In Ref. [18], the social spider optimizer has been presented for determining the optimal size of

MGs. The energy cost has been considered as an objective function. In Ref. [19], energy and power autonomy, payback period, and capital costs aim to be a multi-objective function. Azimuth angle, converter ratings, capital investment, and electricity tariff have been chosen as variables. A two-stage stochastic MILP method has been applied for determining the optimal size of MGs [20]. The economic benefits and resilience performance has been considered as the objectives. In Ref. [21], a nonlinear optimization method has been presented to investigate the battery size to support a grid-connected and standalone grid. Also, in Ref. [22], Mixed-Integer Nonlinear Programming (MINLP) has been proposed for planning MGs. The probability density functions of load and output power of MGs have been integrated into the model.

Recently, Demand Response (DR) programs are suggested for energy efficiency enhancement and operation cost reduction of the MGs. Various projects have been carried out to solve the optimal energy management of MGs with demand response. In Ref. [23], capacity sizing and operation scheduling of isolated MG, considering demand response, have been evaluated. Dynamic pricing has been considered for improving the flexibility of the system. A direct load control DRP has been proposed in Ref. [24] for satisfying the reliability index in MGs. In Ref. [25], minimization of the diesel generator fuel consumption has been considered as an objective function. To overcome this challenge DR plan has been presented.

As aforementioned, due to the intermittent property of RES, generated power in MGs depends on weather and climate conditions. This fact causes an increasing complexity of the consumption-generation balance problem. ESS could reduce the uncertainties nature of RES by storing and releasing the energy. Hence, Optimal scheduling of the ESSs and RESs is one way to reduce the cost and uncertainty of MGs. A complete review of the issues related to energy storage systems in active networks has been provided in Ref. [26]. The location, measurement, economic, social effects, energy security, planning, and implementation of energy storage resources in the main networks have been investigated. The sizing and placement of battery power systems and wind turbines to reduce cost and loss are presented [27]. In Ref. [28], the location and daily charge/discharge of ESS are investigated in the active distribution networks with integrated PV systems. The results show that the over-voltage and energy losses are reduced by using the storage. Also, environmental pollution is decreased, and economic profitability is increased. In Ref. [29], different ESS has been

considered and the operation of the proposed system in combination with electrical and thermal demand-response programs and the three-mode CAES (TM-CAES) unit has been evaluated.

The load supply is the main priority of the system, even under any circumstances. In this paper, a reliable HMGS is proposed to electrify a remote area. Regarding the potential of this region for wind and solar power harvesting, the proposed MG includes the WT/ PV/ ESS. For this aim, wind speed data, which have been collected for 10 years, are utilized. Monte Carlo statistical strategy with autocorrelation is used to estimate wind speed. Also, this method is compared with the Weibull probability density function. The objective of the optimization is total cost-minimizing with satisfying the constraints. Besides the conventional constraints such as environmental and operational ones, other new constraints such as the available budget and available area constraints are considered.

Four days of the year (one day per season) are considered to investigate the seasonal effects. Also, the load shifting DRP is implemented in MG operation. Finally, the number of optimum PV panels, WTs, and ESS are determined. The proposed MG can supply the remote area load by renewable sources without the diesel generator for the whole year. In other words, the proposed MG is environment friendly. The main contributions of this paper can be summarized as follow.

1. The studied system is an environment-friendly isolated HMGS, including PV/wind/ESS, which is design for a remote area at Khalkhal-Iran.
2. The seasonal weather information of Khalkhal is used as a case study for evaluating the distribution of wind speed and output power of solar irradiance.
3. Wind speed distribution and solar radiation are estimated by Monte Carlo simulation. It is based on the past metrological data and considering autocorrelation effects.
4. MILP model is presented for optimal scheduling considering technical and economic ties to find the component size and energy management.
5. The demand response program is applied in HMGS. Its effects are investigated on operation cost, charge and discharge of the ESS, and renewable source efficiency.

This paper is structured as follows. Wind speed estimation is presented in section 2. Section 3 and 4 give the construction of HMGS and optimization problem formulation. In sections 5 and 6, the input data model and MILP optimization results are presented and discussed.

2. THE STATISTICAL METHOD FOE WIND SPEED ESTIMATION AND SOLAR RADIATION

2.1. MC simulation for Wind speed

Many researchers have discovered that wind speed is the most critical parameter of wind power. Therefore, an appropriate determination of the wind speed distribution function is an essential parameter to measure before measuring the wind-harvested energy. Researchers have suggested numerous probability density functions (PDF). One of the most frequently utilized distribution is the Weibull distribution [30]. The Weibull distribution can be presented as follow:

$$p(v) = \left(\frac{A}{k^A} (v^{A-1}) \right) \exp \left(- \left(\frac{v}{k} \right)^A \right) \quad (1)$$

where v is the wind speed, A is the shape factor (unit of speed), and k is the dimensionless scale parameter.

As aforementioned, the wind speed has an intermittent nature and changes annually and seasonally. Hence, using statistical methods to simulate the wind speed should be more effective than the Weibull method. In Weibull results, each estimated value is independent of all other values, and the autocorrelation of data is not considered. MC method and the statistical characteristics of wind speed like autocorrelation are assumed to obtain an appropriate model in this paper. The advantage of this method is its simplicity and generality. It can be used in each site with the past meteorological data of wind speed [31]. For estimation of wind distribution by MC, the following steps have been considered:

1. Past wind speed data acquisition of the site.
2. Calculation of Autocorrelation for 12 months of wind speed data. Fig. 1 shows one sample of the autocorrelation in July in the mentioned site.
3. Finding the repeating patterns in wind data and autocorrelation becomes non-influential for lag d . The smallest lag, under 0.02, is determined as the lag where the autocorrelation becomes none influential.
4. Regrouping wind speed data's at the site into D-day blocks. Therefore, instead of simulation wind speed data independently, correlated wind speed data will be simulated.
5. Each year is divided into $(365/D)$ blocks.
6. N years of actual wind data for the intended site are considered.
7. Scenarios are obtained by sampling from the corresponding blocks in the previous N years.
8. Each of the $365/D$ blocks is sampled from the corresponding blocks in the past N years for L (at least 1000) times, within a year. The sampling is

performed with equal probability equation $(1 / N)$.

9. Finally, we have matrices with L in 52560 ($365 \times 24 \times 60$) dimensions, in which the correlation of the N years data are maintained.

Fig. 2 and 3 show the MC and Weibull simulation versus real data at the site. The probability density of the MC simulation presents an excellent fit to real data. Also the neuro-fuzzy simulation, machine learning method, has been used to compare the results in Fig. 4. In the Weibull and neuro-fuzzy simulation curve, a slight deviation at the top is more than the MC simulation. The benefits of MC are the speed of response and accuracy of using real data and the correlation between data. This method is based on real wind data. As the meteorological data is measured as data with a specific period and is discrete, the estimation fluctuations increase with measurement frequency increasing. As the number of data increases, these fluctuations will be decreased. MC simulation shows the marginal pdf of the simulated samples gives a good match to the pdf of the observed data. The benefits of MC are fast response and accuracy. The reasonable estimate estimation of the MC method is due to correlated data. The statistical properties of the MC, Weibull and neuro-fuzzy method are calculated and summarized in Table 1. The results validate that the MC wind speed simulation is in good agreement with the observed data.

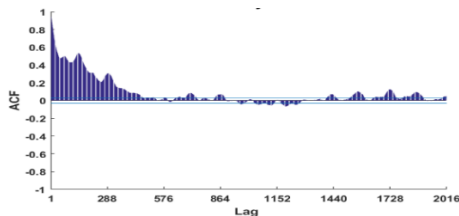


Fig. 1. The autocorrelation of wind data in July

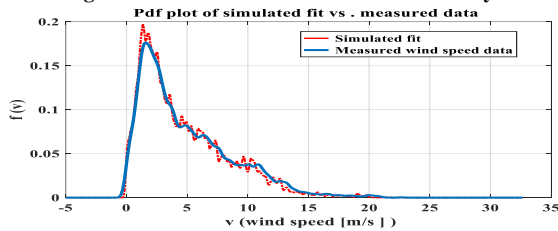


Fig. 2. The Monte Carlo simulation result

Table 1. The statistical results

	Mean[m/s]	Median [m/s]	Std [m/s]
Weibull simulation	8.50	7.73	5.09
Monte Carlo simulation	8.51	8.00	4.99
Neuro-fuzzy simulation	8.57	8.15	4.94
Measured wind speed	8.53	8.04	4.98

Table 2. The statistical results

	Mean[m/s]	Median [m/s]	Std [m/s]
The Monte Carlo simulation	267.059	83	314.125
Measured solar radiation	267.19	84	314.188

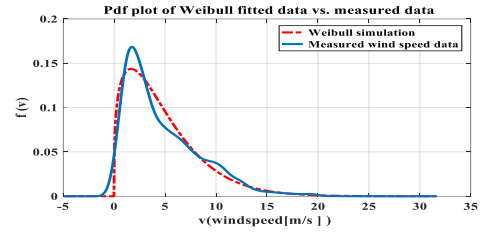


Fig. 3. The Weibull simulation results

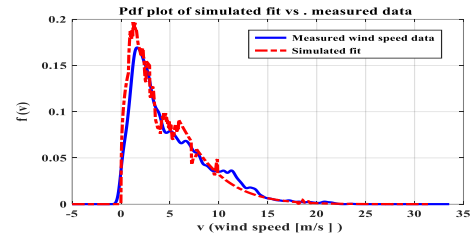


Fig. 4. The Neuro-fuzzy simulation results

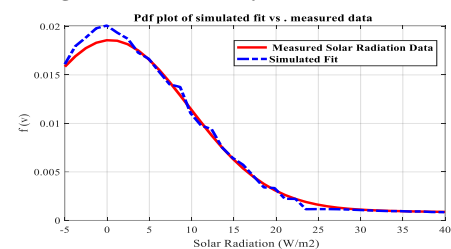


Fig. 5. The Monte Carlo simulation result for solar radiation

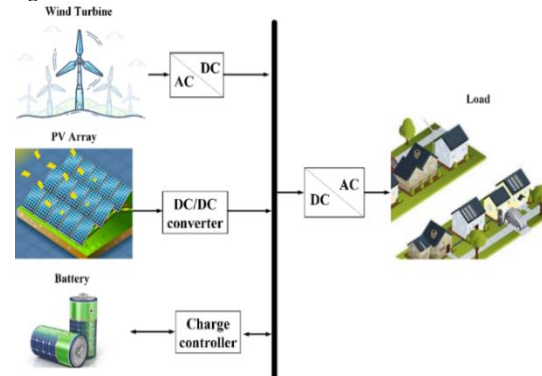


Fig. 6. The Schematic of the hybrid MG

2.2. MC simulation for Solar radiation

The modeling, simulation, and analysis of PV is an essential phase before mount PV system at any location. The operating properties and performance of PV systems are unpredictable due to the solar radiation variation. Therefore in this section the statistical method for solar radiation considering weather variability is proposed based on the MC simulation. The model uses the statistical characteristics of solar radiation like autocorrelation to obtain an appropriate model. The simulation process is similar to wind speed simulation. The simulation results in Fig. 5 and Table 2 show that the proposed model provides accurate model.

3. THE MODEL OF HMGS

The HMGS consists of the production and consumer subsystems. In this configuration, PV panels and WTs

are used for generating energy, as production subsystems, and ESS (battery). If the generation of a hybrid system is not enough to satisfy the load, the power stored in batteries discharged to meet the total energy. The schematic configuration of MG is shown in Fig. 6. It is a low-voltage distribution network to supply 220 V, 50 Hz, AC electricity. Each part of the grid is explained with details in the continuation.

3.1. PV panels

The extractive power of PV is dependent on the solar radiant intensity, panel area, cell temperature, and absorption capacity, which is calculated as following [32-34]:

$$P_{pv-out} = P_{N-pv} \times \frac{G}{G_{ref}} \times [1 + K_t ((T_{amb} + (0.0256 \times G)) - T_{ref})] \quad (2)$$

where P_{pv-out} (kW) is the output power of PV, G_{ref} is reference radiation equal to 1000 W/m², T_{ref} is 25 centigrade, P_{N-pv} is rated power under reference conditions, G is solar radiation (W/m²), K_t is the temperature coefficient of the PV panel which considered $-3.7 \times 10^{-3} (1/^\circ\text{C})$ and T_{amb} is the ambient temperature.

3.2. Wind generation

The aerodynamic characteristics of WT, such as wind speed, specify the output power of WT. A linearized equation of WT power is as following [35]:

$$P_w(t) = \begin{cases} 0, & v \leq v_{cut-in} \text{ OR } v \geq v_{cut-out} \\ P_r \left(\frac{v^3 - v_{cut-in}^3}{v_r^3 - v_{cut-in}^3} \right), & v_{cut-in} < v \leq v_r \\ P_r, & v_r < v \leq v_{cut-out} \end{cases} \quad (3)$$

where, v is the wind speed at turbine hub altitude, v_r nominal speed, v_{cut-in} , and $v_{cut-out}$ are cut-in and cut-out speeds.

3.3. Energy storage

In hybrid energy systems, energy storage devices store energy during high generation and low consumption and provide energy during low generation and high consumption. The battery capacity is calculated by the following equation:

$$S_{batt} = \frac{\text{load average}}{\text{dod} \times \eta_{inv} \times \eta_{bat}} \quad (4)$$

where dod is the depth of charge, η_{inv} is inverter efficiency, and η_{bat} is battery efficiency. Therefore the maximum charge quantity of the battery bank ($E_{bat,max}$) takes the value of battery capacity (S_{batt}) and the minimum charge quantity of the battery bank ($E_{bat,min}$) are obtained as following [36]:

$$E_{bat,max} = S_{batt} \quad (5)$$

$$E_{bat,min} = S_{batt} \times (1 - dod) \quad (6)$$

4. OPTIMIZATION PROBLEM FORMULATION

The planning, integration, and operation of HMGS are complicated because of the higher cost and stochastic nature. Therefore, it is essential to determine the proper sizes of HMGS and connected ESS for effective, economical, and secure operation. The mathematical formulation is discussed in this section.

4.1. Objective function

The short-term scheduling problem of MG is expressed as a MILP. The objective function comprised capital cost (a cost incited on the buying of land, structure, and facilities at the start of the project) and the cost related to operating and maintaining (the annual cost). The Capital Recovery Factor (CRF) is used to convert the capital cost to the annual capital cost. In this regard, the objective function is as follows:

$$\text{Minimizing } F_{MG.cost} \quad (7)$$

$$F_{MG.cost} = F_{NET.P.cost}^K N^K \quad (8)$$

$$F_{Annual.capital.cost} = F_{capital.cost} \times CRF(i, n) \quad (9)$$

$$F_{annual.cost} = F_{annual.capital.cost}^K + F_{OP.cost}^K + F_{MI.cost}^K \quad (10)$$

$$F_{NET.P.COST}^K = \frac{F_{annua.cost}^K}{CRF(i, n)} \quad (11)$$

$$CRF = \frac{i(1+i)^n}{(1+i)^n - 1} \quad (12)$$

where N is the decision variable consists of the values of the size, and the power output of the components of MG (WTs, PVs, and ESSs) over a 24h time interval. $F_{MG.cost}$ is the total cost of the k th component, $F_{capital.cost}$ is the capital cost of the k th component, $F_{OP.cost}$ is the operation cost of the k th component, $F_{MI.cost}$ is the maintenance cost of the k th component, $F_{annual.capital.cost}$ is the annual capital cost of the k th component, and $F_{NET.P.cost}$ is the net present cost of the k th component. i is the real interest rate, and n is the system life period. It is usually equivalent to the life of the PV panel, because of its long life expectancy as compared to other components of HMGS.

4.2. Constraints

The following constraints must be considered to solve the optimization problem.

- **Kirchhoff law or system power balance:**

The generated power and consumption power should be equal for the stable power system.

$$N_{WT}(t) \times P_{WT}(t) + N_{PV}(t) \times P_{PV}(t) + P_d(t) = P_{load}(t) + P_c(t) \quad (13)$$

where $N_{WT}(t)$, $N_{PV}(t)$ are the number of WT, and the number of PVs, respectively. $P_{WT}(t)$ and $P_{PV}(t)$ are the rated power of WT, and PVs. $P_c(t)$ and $P_d(t)$ are the charge and discharge power, and $P_{load}(t)$ is the load power.

• **Energy storage constraints:**

The constraints of ESS are considered as follows:

$$SOC(t) = SOC(t-1) + P_c(t)\eta_c - P_d(t) / \eta_d \quad (14)$$

where $SOC(t)$ and $SOC(t-1)$ are the ESS state of charge (SOC) at the times t and $t-1$, respectively. η_c is the charging efficiency and η_d is the discharging efficiency.

The initial SOC, the constraints of charge and discharge are as follow:

$$SOC(0) = SOC_b \times E_b \max \quad (15)$$

$$SOC(t) = N_b \times E_b \max \quad (16)$$

$$SOC(t) = N_b \times E_b \min \quad (17)$$

where SOC_b is 0.2, and E_{bmax} is the maximum capacity of ESS. $SOC(0)$ is the initial state of charge. N_b is the number of ESS. Eqns. (18)-(19) prevent the synchronous charge and discharge of the ESS:

$$P_c(t) \leq M \times ieec(t) \quad (18)$$

$$P_d(t) \leq M \times ieed(t) \quad (19)$$

$$ieec(t) + ieed(t) \leq 1 \quad ieec \text{ and } ieed \in \{0,1\} \quad (20)$$

M is the large positive number; $ieec$ and $ieed$ are the charge and discharge status of ESS at the time t , respectively.

• **Economic constraints:**

Cost limitation of PV panels, WTs, and energy storage is considered, which the installation cost of components should not exceed assuming maximum available budget:

$$f_{capital.cost.pv} \times N_{pv} + f_{capital.cost.b} \times N_b + f_{capital.cost.WT} \times N_{WT} \leq C_{bg} \quad (21)$$

C_{bg} is the maximum available budget.

• **Land availability constraints:**

Land availability estimations are important in assuming the boundaries to the development of WT and PV. Therefore, these constraints are considered:

$$N_{wind} \times A_b \leq A_{max} \quad (22)$$

$$N_{pv} \times S_b \leq S_{max} \quad (23)$$

where A_b and S_b are the base ground area, A_{max} and S_{max} are the available area for WT and PV, respectively.

• **Capacity constraints of MGs:**

N_{PV}^{\min} , N_{PV}^{\max} , N_{WT}^{\min} , and N_{WT}^{\max} are the minimum and maximum number of the WTs and PVs. These can be calculated as follow. α , β , γ , and λ are scaling factors.

$$N_{PV}^{\min} = \frac{\alpha \sum_{t=1}^{24} P_L(t)}{\sum_{t=1}^{24} P_{PV}(t)}, \quad N_{PV}^{\max} = \frac{\beta \sum_{t=1}^{24} P_L(t)}{\sum_{t=1}^{24} P_{PV}(t)} \quad (24)$$

$$N_{WT}^{\min} = \frac{\gamma \sum_{t=1}^{24} P_L(t)}{\sum_{t=1}^{24} P_{WT}(t)}, \quad N_{WT}^{\max} = \frac{\lambda \sum_{t=1}^{24} P_L(t)}{\sum_{t=1}^{24} P_{WT}(t)} \quad (25)$$

4.3. Load shifting demand response program (LS-DRP)

Demand Response programs are the group of methods for reducing or shifting electricity consumption at the demand side. Generally, it can be defined as the method for improvement of the energy system at the side of consumption. The goal of LS-DRP is to minimize the peak load and move them to off-peak hours. As a result, the load profile will be flat and causes lower total operating costs. This demand elasticity (E) is corresponded to electricity price (EP) and defined as:

$$E = \left(\frac{EP_0}{P_{L0}} \right) \left(\frac{\partial P_L}{\partial EP} \right) \quad (26)$$

where EP_0 and P_{L0} are primary electricity price and load demand respectively. ∂EP and ∂P_L demonstrate the variation in electricity price and load demand from their primary values respectively. Inflexible loads cannot shift their request from one period to another with the price variation. They are sensitive to a single period only and are named as self-elasticity. Moreover, some flexible loads that can change from peak hours to low load periods having sensitivity to multi-period can be defined as cross flexibility. To consider the DR the following equation is attached to the model stated in Section 4.1, as

$$P_{Load}(t) = D_{ref}(t) + DR^{up}(t) - DR^{do}(t) \quad (27)$$

where D_{ref} is demand submitted by the load at the time t without demand response; DR^{up} demand increase of load at the time t due to demand response, DR^{do} demand decrease of load at the time t due to demand response.

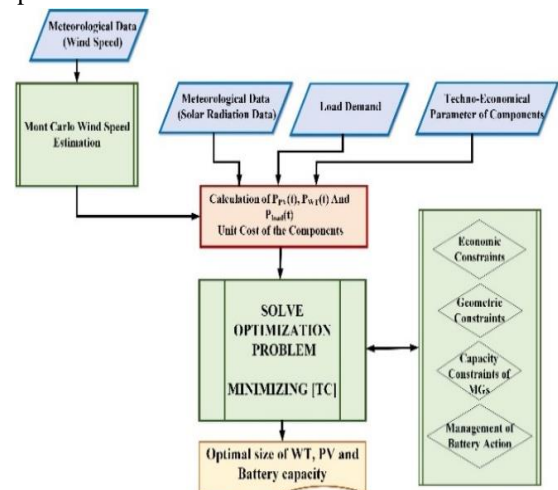


Fig. 7. Generalization of the proposed method

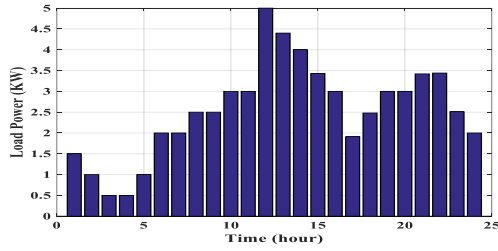


Fig. 8. Daily load profile

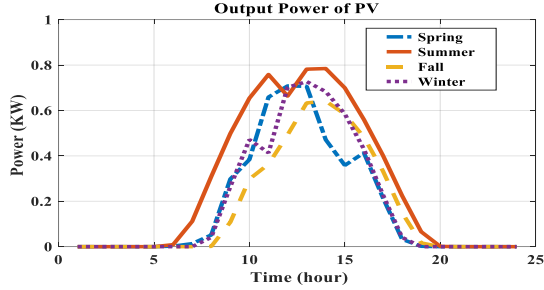


Fig. 9. Power supplied by the panels

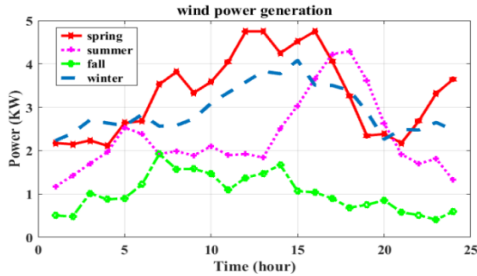


Fig. 10. Mean wind power generation

Table 3. MG utilized components

Wind	
V_{CUT-IN}	2.5 m/s
$V_{CUT-OUT}$	13 m/s
$C_{int-wind}$	3200\$/unit
v_r	9.5 m/s
P_r	5 kw
CC_{Wind}	3200 \$/unit
$OP_{wind} \& MI_{wind}$	100 \$/year
Life span	20 years
Available area for wind	80 m ²
PV	
P_N^{PV}	1 kw
$OP_{PV} \& MI_{PV}$	5 \$/year
CC_{PV}	1800\$/unit
Life span	25 year
η_{PV}	0.85
Available area for PV	1.7
C_{int-pv}	1800\$/unit
Budget available	5000000\$
η_{inv}	0.95
i (interest rate)	0.06
Battery	
Voltage	12v
$E_{b,max}$	70 kwh
$E_{b,min}$	13.2 kwh
η_{bat}	85%
CC_{bat}	130\$/unit
Life span	5 years
dod	0.8
soc_0	13.2kwh
$OP_{bat} \& MI_{bat}$	5 \$/year
$C_{int-bat}$	130\$/unit

5. CASE STUDY

The general structure of the proposed method is summarized as a flowchart in Fig. 7. Weather and geographical data of Khalkhal are applied to study the scheduling of HMGS. Khalkhal is located in the northwest of Iran and extends on the geographical coordinates of 37° 37' 08" N 48° 31' 33" E. Khalkhal is in one of the coldest areas in Iran. Essential meteorology data of Khalkhal are presented in Refs. [37-38]. Four days of a year (one day per season), which correspond to the conditions of wind speed and solar radiation in their season, are investigated to obtain the amount of power produced in these seasons. Fig. 8 shows the hourly load profile with 5 kW peak load. The grid supplies 15 households. Techno-economical features of HMGS are tabulated in Table. 3. Fig. 9 and 10 show the PV output power and WT power generation in different seasons in the mentioned site.

6. RESULTS AND DISCUSSION

The power management strategy for HMGS is performed by GAMS software and the MILP method. The objective function is the cost-minimizing to achieve the most suitable configuration of the system and the continuous electrification. The solution deals with the optimum size of the grid components. By considering the maximum and minimum number of MGs, which stated in the previous section, the minimum number of WT and PV have resulted in 10 and 50, and the maximum number are 65 and 170, respectively. To emphasize on the budget and available area constraints effects on MG size optimization, also to evaluate MG scheduling with DR, 3 different scenarios are simulated.

Scenario1: Cost minimization without considering the budget and available space constraints.

Scenario2: Cost minimization by considering all constraints.

Scenario3: Cost minimization by considering all constraints and demand response.

One sample day in each season of the year is considered for seasonality variability of wind speed and solar radiation. In this short-term planning problem, because of choosing four days, which represent four seasons in a year, there is no continuity between days. So, energy interchange between ESS and the load-generation system must be settled in each day. The results show that MILP provides optimum wind, PV, and ESS ratings. The obtained results and associated costs are presented in Tables 4 and 5. The optimization results for the sample days are shown in Figs. 11 to 18.

Table 4. Optimal component size and total cost for scenario 1

scenario 1				
	Spring	Summer	Fall	Winter
Number of WT	10	20	65	15
Number of PV	55	153	170	140
ESS	2	2	2	2
Cost (×103\$)	1022.795	1065.678	1079.790	1053.253

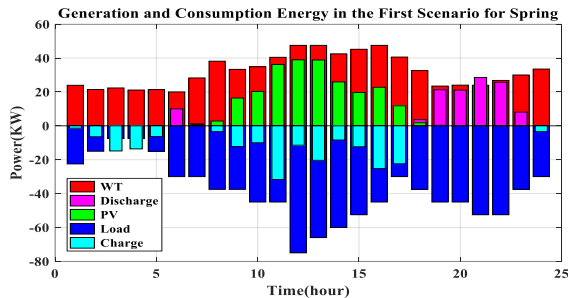


Fig. 11. Generation and consumption power in Sci. 1 for spring

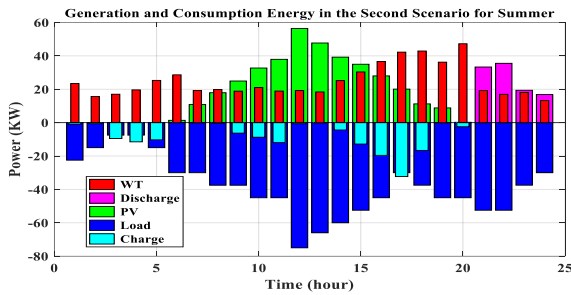


Fig. 12. Generation and consumption power in Sci. 1 for summer

Fig. 11 shows the power profiles during the spring season, where 10 WTs, 55 solar panels, and 2 ESS are installed. During this season, the wind speed is very high (more than 12 m/s). Also, it exists during the night, when the PV system does not generate electricity. Thereby, The PV provides up to 20 % of the total requested energy. WT provides a significant portion of the total energy demand. The ESS provides 10 % of the total energy at night. ESS is charged during the day when the wind turbine generates power more than the demand and is discharged at night, when the wind speed is lower. Fig. 12 shows the power profiles during the summer season. The length of the night and day are approximately the same in summer and spring, but the wind speed conditions in this season are not favorable, as shown in Fig. 10 So, the number of WTs is increased to 20. WTs produce 55% of the total energy. Nevertheless, summer radiation is the most favorable weather conditions. Days are long, and PV panels produce 35% of total energy. Thereby, 2 ESS units are used to store energy during the day and discharge during the night.

Fig. 13 shows the results of the fall season. During the fall season, the optimization solution recommends that using 65 WTs, 170 panels, and 2 ESS units. Due to the low energy generation of PVs during cloudy days in

the fall, the number of recommended WTs is the highest for this season. Wind power produces 53% of the total generation. Also, besides, days start getting smaller, and PVs produce 40 % of the generation. 7 % of total energy is consumed by charging ESS during the day that PV and wind generate power. Also, discharging happens at night when PV does not provide power. Fig. 14 shows that during the winter season, 15 WTs are sufficient for satisfying load consumption. Moreover, 140 PV panels must be installed. ESS units compensate for low PV production similar to the fall, but wind generation is more than the generation of fall. It is essential to mention that the budget and area constraints have not been considered for the results, which are achieved so far.

In the following, the results of scenario 2, which includes comprehensive constraints, are presented. MILP yields component size and related costs for this scenario, which are given in Table 5. According to these results, Figs. 15 to 18 show the energy balance of MG for all seasons. In terms of net consumption and the energy storage constraints, simulation results are presented in Tables 6 and 7 for the spring in two scenarios.

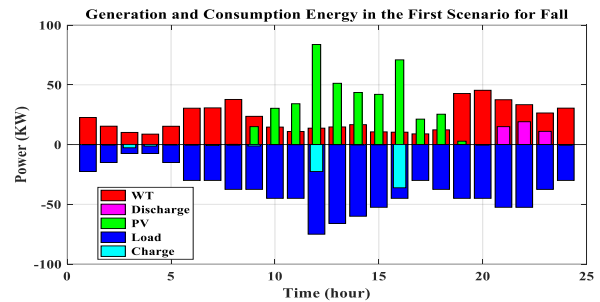


Fig. 13. Generation and consumption power in Sci. 1 for fall

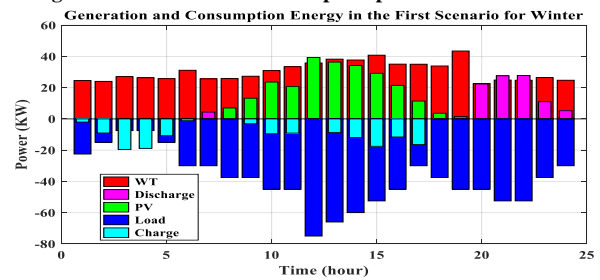


Fig. 14. Generation and consumption power in Sci. 1 for winter

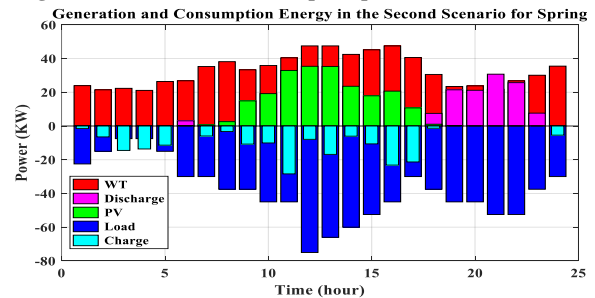


Fig. 15. Generation and consumption power in Sci. 2 for spring

Table 5. Optimal component size and total cost for scenario 2

scenario 2				
	Spring	Summer	Fall	Winter
Number of WT	10	23	64	17
Number of PV	50	134	147	104
ESS	3	2	2	2
Cost ($\times 103\$$)	1019.974	1048.077	1070.824	1026.763

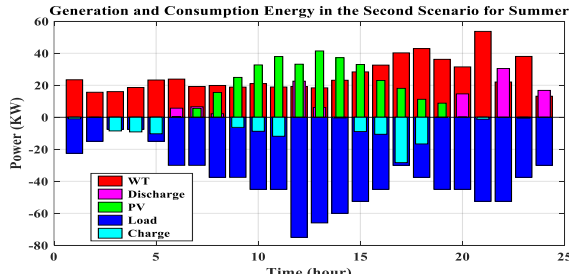


Fig. 16. Generation and consumption power in Sci. 2 for summer

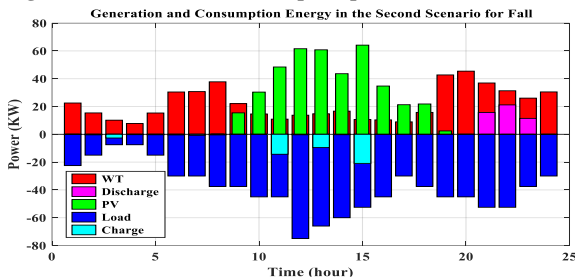


Fig. 17. Generation and consumption power in Sci. 2 for fall

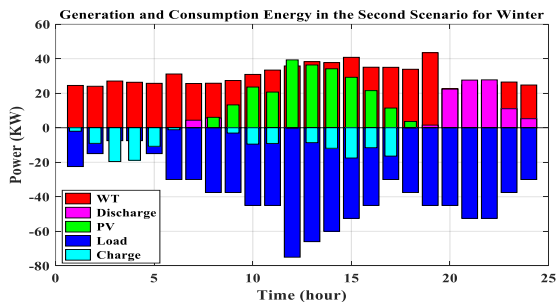


Fig. 18. Generation and consumption power in Sci. 2 for winter

To compare two scenarios, the percentage of power production by PV, WT, and ESS in the scenarios are demonstrated in Fig. 19. Although in both scenarios, the load is satisfied, in scenario-2, WT and PV counts have reduced deals with considering area and budget constraints. It causes to minimize the total cost. The reason for cost reductions in the second scenario is the optimum selection of the number of PV, WT and ESS. As shown in Tables 4 and 5, the number of PV and WT is decreased but the number of ESS is increased. Finally, the last decision for counts of WTs and PVs are 64 and 147. The decision is made based on the worst season of the year with the lowest wind speed and sunshine. Therefore, the total cost is $1070.824 \times 103\$$.

Also, in Table 8, the obtained results are compared by the results of Ref. [39]. As shown, the MILP optimization model produces appropriate sizing and less total cost compared to MOPSO optimization.

Table 6. The numerical result of power generation and consumption in the first scenario for spring season

Time	P_{WT}	P_{PV}	$P_{discharge}$	P_{charge}	P_{Load}
T1	23.9241	0	0	1.4241	22.5
T2	21.46631	0	0	6.4663	15
T3	22.3450	0	0	14.8450	7.5
T4	21.1263	0	0	13.6263	7.5
T5	21.3644	0	0	6.3644	15
T6	20.0082	0.01232	10.007	0	30
T7	28.2632	0.7344	1.12	0	30
T8	38.1443	2.8290	0	3.473406	37.5
T9	33.3279	16.3943	0	12.2223	37.5
T10	34.8573	20.3167	0	9.9892	45
T11	40.4454	36.2458	0	31.6912	45
T12	47.5	38.9472	0	11.4472	75
T13	47.5	38.8625	0	20.3625	66
T14	42.4798	25.9079	0	8.3878	60
T15	45.1859	19.7027	0	12.3886	52.5
T16	47.5	22.7464	0	25.2464	45
T17	40.5859	11.8096	0	22.3956	30
T18	32.5847	1.7879	3.1443	0	37.5
T19	23.4552	0.2905	21.2541	0	45
T20	24.0152	0	21.0942	0	45
T21	23.9396	0	28.5603	0	52.5
T22	26.8009	0	25.6990	0	52.5
T23	30.0111	0	7.0624	0	37.5
T24	33.5093	0	0	3.4241	30

Table 7. The numerical result of power generation and consumption in the second scenario for spring season

Time	P_{WT}	P_{PV}	$P_{discharge}$	P_{charge}	P_{Load}
T1	23.9241	0	0	1.4241	22.5
T2	21.4663	0	0	6.4663	15
T3	22.3450	0	0	14.7883	7.5
T4	21.1263	0	0	13.6263	7.5
T5	26.3644	0	0	11.3644	15
T6	26.8243	0.1120	3.0635	0	30
T7	35.2632	0.6676	0	5.9308	30
T8	38.1443	2.5718	0	3.2162	37.5
T9	33.3279	14.9039	0	10.7319	37.5
T10	35.8573	19.1970	0	10.0543	45
T11	40.4454	32.9507	0	28.3961	45
T12	47.5	35.4066	0	7.9066	75
T13	47.5	35.3296	0	16.8296	66
T14	42.4798	23.5527	0	6.0325	60
T15	45.1859	17.9115	0	10.5974	52.5
T16	47.5	20.6786	0	23.1786	45
T17	40.5859	10.7360	0	21.3220	30
T18	30.5847	1.0625	7.4812	1.3220	37.5
T19	23.4552	0.0854	21.4592	0	45
T20	23.8152	0	21.1847	0	45
T21	21.7632	0	30.7367	0	52.5
T22	26.8009	0	25.6990	0	52.5
T23	30.1113	0	7.6241	0	37.5
T24	35.5093	0	0	5.4241	30

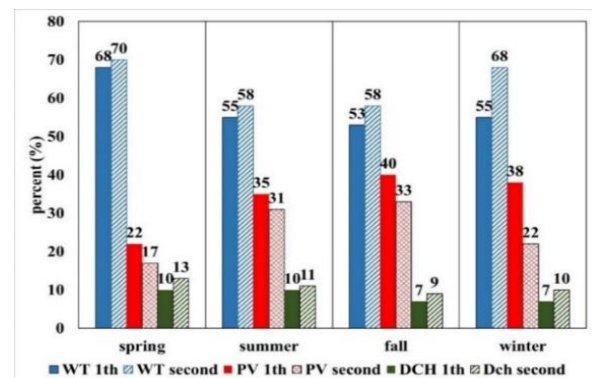


Fig. 19. Percentage of generated power by HMGs in the scenarios

By considering the two scenario results, an essential portion of the generation is WT, which is dependent on the wind speed. Fig. 20 shows wind power generation of all-season in scenario 1. As the results show, the worst season in wind generation is fall, and this season determined the optimal number of MGs. Therefore, the precise estimation of wind power is a critical problem in the power scheduling of HMG. As shown in the results, the implementation of more constraints in the simulation significantly optimized the results. The energy stored in ESS increased in the second scenario, and it causes the number of PV and WT to reduce. Also, this can reduce operation and maintenance costs associated with the WT and PV.

Table 8. Comparing the total cost by [39]

	Nahavand [39]	Rafsanjan [39]	Khash [39]	Khalkhal
Cost \$/kWh	1.87	0.32	0.35	0.148

Table 9. Total Cost with and without DR, scenario 3

	Total Cost	
	Without DR	With DR
Cost (×103\$)	1070.824	1021.719

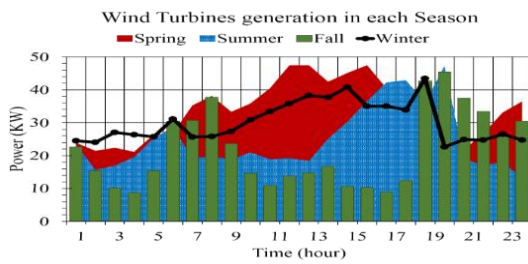


Fig. 20. The wind power generation in the first scenario

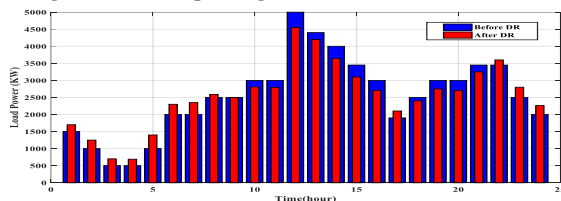


Fig. 21. Consumed loads profiles (with and without DR)

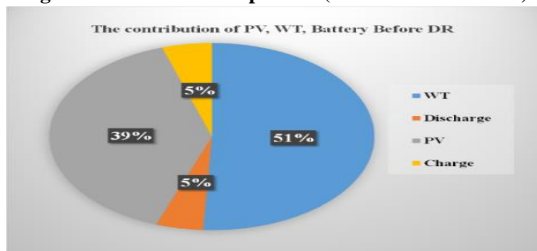


Fig. 22. The contribution of HMGS without DR, scenario 3

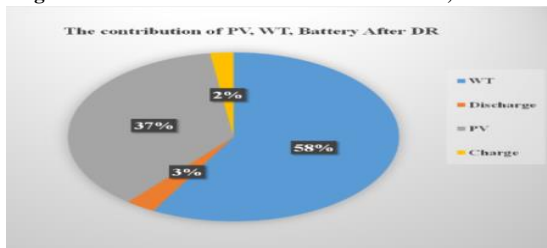


Fig. 23. The contribution of HMGS with DR, scenario 3

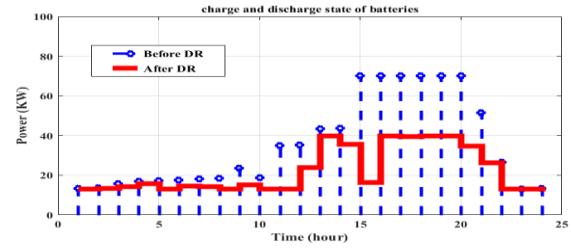


Fig. 24. The charge and Discharge states of batteries with and without DR, scenario 3

In scenario 3, the simulation and results of MG optimization with DR are presented in the fall season which is the worst season in the viewpoint of the weather condition. Fig. 21 shows the impact of running LS-DR on the load profile. As shown in this figure, by implementing the DRP, peak loads are reduced and the loads are shifted to other periods (mid-load and low load period). Fig. 22 and 23 illustrate the percentage of participation of RESs and ESSs in covering the load after and before DR, respectively. By the proposed methodology the PV system covers 39% of the load while 51% of the required energy will be covered via the WT. Also, batteries participate by 10% of the demand power before DR. While, after DR, shifting load can be an opportunity to increase wind penetration in the system and improve its management. Therefore, the PV system, WT, and batteries cover 37%, 58% and, 5% of the demand power after DR. Also, as presented in Table 9, the total operational cost of MGs in the case, which the DR is run, is \$1021.719. It is less than the cost of without DR condition.

The charge state and discharge state of batteries in cases without DR and with DR are shown in Fig. 24. As illustrated, the total amount of the charging/discharging active power in the case with DR is less than the case without DR. As mentioned before, batteries saved the energy in off-peak hours and injected it into the MG during peak hours. Therefore, by implementation DR and shifting the loads, the stored energy will be reduced significantly. The simulation results demonstrate that the proposed energy management with the implementation of DR not only decreases the operational costs but also decreases the stored energy. It causes to increase the MG efficiency.

7. CONCLUSION

The penetration of renewable energy sources in electrification with its advantages in the field of environmental pollution and reduction of dependence on fossil fuel sources offers important challenges for energy networks. These issues need to be addressed by appropriately energy management, sizing of RES along with BESS due to their alternate nature of solar, and

wind energy resources. For determining the optimal size of PV, WT, and energy storage, a MILP formulation has been proposed based on flexible demand response. A novel stochastic method for the prediction of wind power using Monte Carlo scenarios is presented. The outputs of the appropriate size of HMGS and overall cost of the system are indicated the proper performance of the proposed strategy despite all strict constraints such as geometric constraints, climate changes, capacity constraints of RES, and demand response management constraints. The DR program cause to minimize the total MG cost as well as the stored energy of batteries. Also, it maximizes RES harvesting and MG efficiency. The same approach can be executed for each remote area to plan and design hybrid MG.

REFERENCES

- [1] A. Diab et al., "Application of different optimization algorithms for optimal sizing of PV/wind/diesel/battery storage stand-alone hybrid microgrid", *IEEE Access*, vol. 7, pp. 119223-45, 2019.
- [2] M. Khan, A. Yadav, L. Mathew, "Techno economic feasibility analysis of different combinations of PV-wind diesel-battery hybrid system for telecommunication applications in different cities of Punjab, India", *Renew. Sustain. Energy Rev.*, vol. 76, pp. 577-607, 2017.
- [3] A. Agüera-Pérez et al., "Weather forecasts for microgrid energy management: review, discussion and recommendations", *Appl. Energy*, vol. 228, pp. 265-78, 2018.
- [4] R. Jane et al., "Characterizing meteorological forecast impact on microgrid optimization performance and design", *Energies*, vol. 13, pp. 577, 2020.
- [5] A. Khosravi et al., "Prediction of wind speed and wind direction using artificial neural network, support vector regression and adaptive neuro-fuzzy inference system", *Sustain. Energy Tech. Assess.*, vol. 25, pp.146-160, 2018.
- [6] G. Osório, J. Matias, J. Catalão, "Short-term wind power forecasting using adaptive neuro-fuzzy inference system combined with evolutionary particle swarm optimization, wavelet transform and mutual information", *Renew. Energy*, vol. 75, pp.301-7, 2015.
- [7] O. Karakuş, E. Kuruoğlu, M. Altinkaya, "One-day ahead wind speed/ power prediction based on polynomial autoregressive model", *IET Renew. Power Gener.*, vol. 11, pp. 1430-9, 2017.
- [8] M. Alamaniotis, G. Karagiannis, "Integration of Gaussian processes and particle swarm optimization for very-short term wind speed forecasting in smart power", *Int. J. Monit. Surveill. Tech. Res.*, vol. 5, pp. 1-14, 2017.
- [9] M. Alamaniotis, G. Karagiannis, "Application of fuzzy multiplexing of learning Gaussian processes for the interval forecasting of wind speed", *IET Renew. Power Gener.*, vol. 14, pp.100-9, 2019.
- [10] F. Nitsch, O. Turkovska, J. Schmidt, "Observation-based estimates of land availability for wind power: a case study for czechia", *Energy Sustain. Soc.*, vol. 9, pp. 1-13, 2019.
- [11] A. Santos et al., "Framework for microgrid design using social, economic, and technical analysis", *Energies*, vol. 11, pp. 2832, 2018.
- [12] H. Hosseinnia, B. Tousi, "Optimal operation of dg-based micro grid (MG) by considering demand response program (DRP)", *Electric Power Syst. Res.*, vol. 167, pp. 252-60, 2019.
- [13] B. Dey et al., "Solving energy management of renewable integrated microgrid systems using crow search algorithm", *Soft Comput.*, vol. 22, pp. 55-66, 2019.
- [14] F. El-Faouri et al., "Modeling of a microgrids power generation cost function in real-time operation for a highly fluctuating load", *Simulation Modell. Practice Theory*, vol. 94, pp. 118-133, 2019.
- [15] A. Yasmeen et al., "Optimal energy management in microgrids using meta-heuristic technique", *Int. Conf. Emerging Internetworking, Data Web Tech.*, 2018.
- [16] A. Ehsana, Q. Yang, "State-of-the-Art techniques for modelling of uncertainties in active distribution network planning", *Rev. Appl. Energy*, vol. 239, pp. 1509-23, 2019.
- [17] E. Shahryari et al., "A copula-based method to consider uncertainties for multi-objective energy management of microgrid in presence of demand response", *Energy*, vol. 175, pp. 879-90, 2019.
- [18] A. Fathy, K. Kaaniche, T. Alanazi, "Recent approach based social spider optimizer for optimal sizing of hybrid PV/Wind/Battery/Diesel integrated microgrid in aljouf region", *IEEE Access*, vol. 8, pp. 57630-45, 2020.
- [19] S. Bandyopadhyay et al., "Techno-economical model based optimal sizing of PV-battery systems for microgrids", *IEEE Trans. Sustain. Energy*, vol. 11, pp. 1657-68, 2019.
- [20] D. Wu et al., "Stochastic optimal sizing of distributed energy resources for a cost-effective and resilient microgrid", *Energy*, vol. 5, pp. 117284-96, 2020.
- [21] U. Salman, F. Al-Ismael, M. Khalid, "Optimal sizing of battery energy storage for grid-connected and isolated wind-penetrated microgrid", *IEEE Access*, vol. 8, pp. 91129-38, 2020.
- [22] V. Thang, "Optimal sizing of distributed energy resources and battery energy storage system in planning of islanded micro-grids based on life cycle cost", *Energy Syst.*, vol. 8, pp.1-20, 2020.
- [23] M. Kiptoo et al., "Integrated approach for optimal techno-economic planning for high renewable energy-based isolated microgrid considering cost of energy storage and demand response strategies", *Energy Convers. Manage.*, vol. 215, pp. 112917-33, 2020.
- [24] S. Mohseni, A. Brent, D. Burmester, "A demand response centred approach to the long-term equipment capacity planning of grid-independent micro-grids optimized by the moth-flame optimization algorithm", *Energy Convers. Manage.*, vol. 200, pp. 112105-23, 2019.
- [25] A. Dejamkhooy et al., "Fuel consumption reduction and energy management in stand-alone hybrid microgrid under load uncertainty and demand response by linear programming", *J. Oper. Autom. Power Eng.*, vol. 8, pp. 273-81, 2020.
- [26] K. Das Choton et al., "Overview of energy storage systems in distribution networks: placement, sizing, operation, and power quality", *Renew. Sustain. Energy Rev.*, vol. 91, pp. 1205-30, 2018.
- [27] A. Jalali, M. Aldeen, "Risk-based stochastic allocation of ESS to ensure voltage stability margin for distribution systems", *IEEE Trans. Power Syst.*, vol. 34, pp. 1264-77, 2019.
- [28] M. Rasoljannesar et al., "Optimal placement, sizing, and daily charge/discharge of battery energy storage in low

- voltage distribution network with high photovoltaic penetration”, *Appl. Energy*, vol. 226, pp. 957-66, 2018.
- [29] H. Mousavi, M. Jadidbonab, B. Mohammadi, “Stochastic assessment of the renewable-based multiple energy system in the presence of thermal energy market and demand response program”, *J. Oper. Autom. Power Eng.*, vol. 8, pp. 22-31, 2020.
- [30] P. Wais, “A review of weibull functions in wind sector”, *Renew. Sustain. Energy Rev.*, vol. 70, pp. 1099-107, 2017.
- [31] T. Ishihara, A. Yamaguchi, “Prediction of the extreme wind speed in the mixed climate region by using monte carlo simulation and measure correlate predict method”, *Wind Energy*, vol. 18, pp. 171-86, 2015.
- [32] H. Lan et al., “Optimal sizing of hybrid PV/diesel/battery in ship power system”, *Appl. Energy*, vol. 158, pp. 26-34, 2015.
- [33] S. Tito, T. Lie, T. Anderson, “Optimal sizing of a wind-photovoltaic-battery hybrid renewable energy system considering socio-demographic factors”, *Solar Energy*, vol. 136, pp. 525-32, 2016.
- [34] A. Daud, M. Ismail, “Design of isolated hybrid systems minimizing costs and pollutant emission”, *Renew. Energy*, vol. 44, pp. 215-24, 2012.
- [35] L. Wang, C. Singh, “PSO-based multi-criteria optimum design of a grid connected hybrid power system with multiple renewable sources of energy”, *Swarm Intell. Sympos.*, 2007.
- [36] M. Amrollahi, S. Bathaee, “Techno-economic optimization of hybrid photovoltaic/wind generation together with energy storage system in a stand-alone micro-grid subjected to demand response”, *Appl. Energy*, vol. 202, pp. 66-77, 2017.
- [37] Iran Renewable Energy Organization (SUNA) Available At: <<http://www.suna.org/fa/home>>.
- [38] NASA Surface meteorology and Solar Energy-Location Available At: <[https:// eosweb.larc.nasa.gov](https://eosweb.larc.nasa.gov)>
- [39] H. Borhanazad et al., “Optimization of micro-grid system using MOPSO”, *Renew. Energy*, vol. 71, pp. 295-306, 2014.